Chip-Scale Acoustic Resonator Based Oscillators

Mihir Chaudhari, *Student Member, IEEE*, Ruochen Lu, *Senior Member, IEEE*

***Abstract*—This report presents the results of the project on developing chip-scale oscillators based on acoustic resonators. The results in this report cover the first phase of the project, which is developing an acoustic resonator suitable for oscillator use. Here, an S1 mode bulk acoustic wave (BAW) resonator is fabricated on a thin-film lithium niobate platform with a resonant frequency at 5.476 GHz and a *Q* of 243.**

***Index Terms*—acoustic resonators, bulk acoustic wave, thin-film lithium niobate, oscillators**

I. INTRODUCTION

INTEGRATED oscillators play a critical role in electronics; they provide precise timing, synchronization, and frequency generation. These functionalities are vital for communications, computing, and instrumentation [1], [2]. The industry standard for radio frequency (RF) oscillators relies on dielectric-based electromagnetic (EM) resonators or inductor-capacitor (LC) tank solutions [3], [4]. In the RF regime these solutions have high quality factors *Q*s; however, acoustic resonator-based solutions offer more compact solutions because of the shorter acoustic wavelength compared to the EM wavelength at the same frequency (Fig. 1) [5]. The challenges of using acoustic resonators for oscillators are increased loss, phase noise, and achieving a high figure of merit ($f \cdot Q$) above 2 GHz. When scaling down physical dimensions to increase the operating frequency, temperature dependent effects can cause the resonant frequency, *f*, to shift, impacting the overall performance of the oscillator [6]. The proposed project aims to create a single-chip frequency-tunable oscillator that compensates for thermal effects without compromising the signal.

The first step to creating an acoustic resonator-based oscillator is fabricating an acoustic resonator. This report covers the fabrication of the resonator and its characterization. In the proposed project two more components are required: (1) a frequency tuning mechanism with an actuated metal trace tunes the resonant frequency by altering the acoustic wave velocity, and (2) integrated circuit components and a thermistor provide a temperature detection and feedback mechanism to stabilize the oscillator's frequency. Future work on this project will advance these two goals to enable a fully integrated chip-scale acoustic resonator-based oscillator.

Mihir Chaudhari and Ruochen Lu are with the Chandra Family Department of Electrical and Computer Engineering, The University of Texas at Austin, Austin, TX 78712 USA (e-mail: mihirc@utexas.edu).

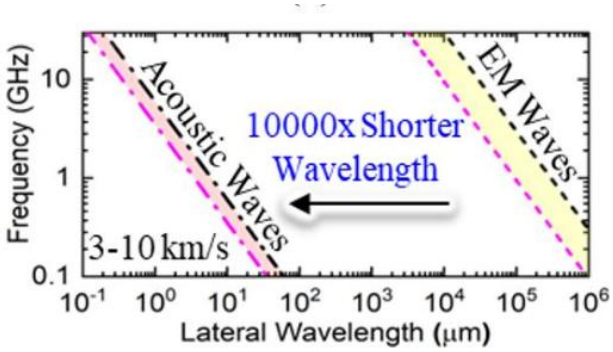

Fig. 1. Comparison of frequencies and wavelengths of acoustic waves and EM waves.

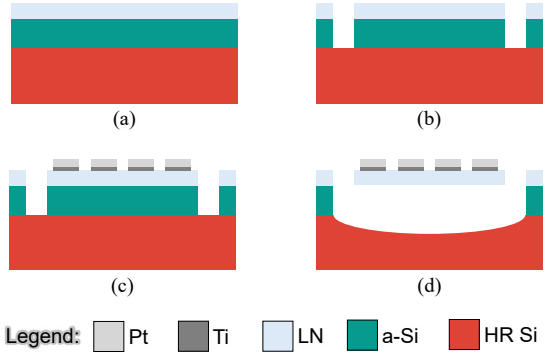

Fig. 2. Resonator fabrication flow schematic. First, the initial stack (a) is etched to create release windows (b) to later suspended the device. Next, metal is deposited on top of the stack (c). Finally, the resonator is suspended with a XeF_2 dry etch.

II. ACOUSTIC RESONATOR FABRICATION

The acoustic resonator is fabricated on a thin-film lithium niobate (LN) platform. LN is chosen for its high electro-mechanical coupling coefficient, which enables overmoding. Overmoding suffers from a drastic coupling (k^2) loss proportional to 1/(square of the mode order), but having a fundamental mode with a large k^2 can enable overmode frequency scaling [7]. The resonator is designed to target the 1st order symmetric S1 acoustic mode. A schematic of the fabrication flow is presented in Fig. 2. The resonator is fabricated on 600 nm X-cut LN on top of 1 μm amorphous Si (a-Si) on top of high-resistivity Si (HR Si). The metals selected for the electrodes are 40 nm of Pt with a 5 nm Ti adhesion layer. The fabrication procedure is as follows: First, release windows are etched through the LN and the sacrificial a-Si layer via Ar gas ion milling. Next, metal is deposited onto the LN by electron beam evaporation in two deposition rounds. First, 5 nm of Ti followed by 40 nm of Pt are deposited for the electrodes. Next, an additional 40 nm of Pt

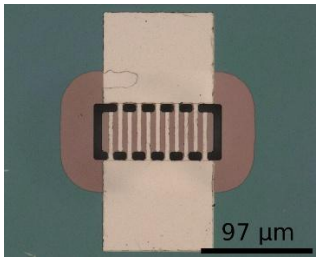

Fig. 3. Optical microscope image of a fabricated S1 mode acoustic resonator on thin-film lithium niobate.

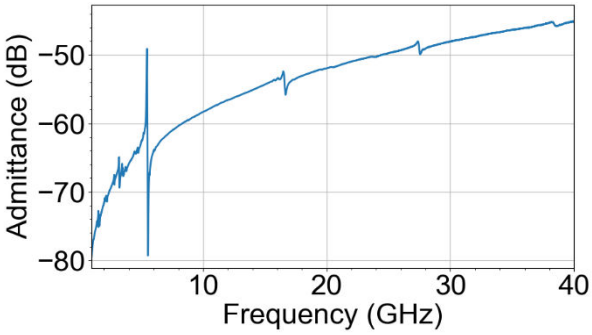

Fig. 4. Measured wideband electrical admittance of the S1 mode resonator from 1 to 40 GHz.

are deposited to thicken the ground-signal-ground (GSG) probe pads. After the metal deposition, the devices are suspended by a XeF_2 dry etch. The resonator after fabrication is shown is Fig. 3.

III. Acoustic Resonator Characterization

The acoustic resonator's electrical performance is characterized by a Keysight vector network analyzer (VNA), and relevant parameters are extracted from the measurement. The measurement is a two-port measurement with two GSG probes. A wideband sweep of the electrical admittance is shown in Fig. 4. And a narrowband sweep of the targeted S1 mode's electrical admittance is shown in Fig. 5. The S1 mode has a resonant frequency of 5.476 GHz and a 3 dB Q of 243.

While the measured S1 mode resonator demonstrates a resonant frequency of 5.476 GHz with a Q of 243, understanding the mechanisms that limit the quality factor is critical for improving performance in future designs. In thin-film lithium niobate bulk acoustic wave resonators, several loss mechanisms contribute to Q degradation, including acoustic radiation loss, material damping, electrode-related loss, and anchor loss due to imperfect suspension.

At high frequencies, acoustic energy leakage into the substrate can significantly reduce Q if the resonator is not sufficiently isolated. Although the device is suspended using XeF_2 etching, residual anchor loss may still occur. Another source of loss is the electrodes. The use of platinum electrodes introduces mass loading and acoustic attenuation that can reduce the effective Q of the resonant mode.

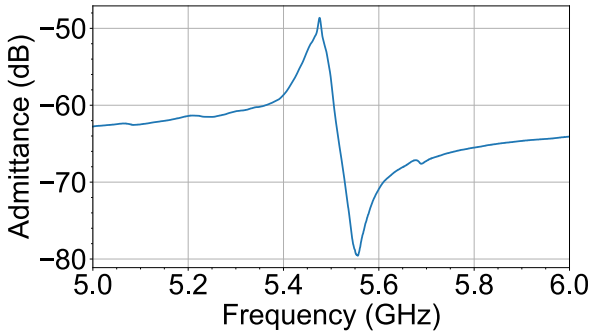

Fig. 5. Measured narrowband electrical admittance of the S1 mode resonance.

Material loss in lithium niobate, including phonon-phonon interactions and thermoelastic damping, also contributes to energy dissipation. These effects become more pronounced at higher frequencies, and can be affected by temperature fluctuations. Improving Q in future iterations may involve optimizing electrode thickness, exploring alternative electrode materials, and refining the suspension geometry to further suppress anchor loss.

Acknowledgment

This work was supported by the IEEE MTT-S Undergraduate Scholarship.

References

[1] Pierce, G. W. (1923). Piezoelectric Crystal Resonators and Crystal Oscillators Applied to the Precision Calibration of Wavemeters. Proceedings of the American Academy of Arts and Sciences, 59(4). https://doi.org/10.2307/20026061E.

[2] el Ftouh, H., Moustapha, E. B., Naima, A. T., & Alia, Z. (2022). Ultra low phase noise and high output power monolithic microwave integrated circuit oscillator for 5G applications. International Journal of Electrical and Computer Engineering, 12(3). https://doi.org/10.11591/ijece.v12i3.pp2689-2698R.

[3] Ullah, U., Ain, M. F., & Ahmad, Z. A. (2017). A review of wideband circularly polarized dielectric resonator antennas. In China Communications (Vol. 14, Issue 6). https://doi.org/10.1109/CC.2017.7961364

[4] Trinh-Van, S., Yang, Y., Lee, K. Y., & Hwang, K. C. (2016). A wideband circularly polarized pixelated dielectric resonator antenna. Sensors (Switzerland), 16(9). https://doi.org/10.3390/s16091349.

[5] E. T. . -T. Yen et al., "Integrated High-frequency Reference Clock Systems Utilizing Mirror-encapsulated BAW Resonators," 2019 IEEE International Ultrasonics Symposium (IUS), Glasgow, UK, 2019, pp. 2174-2177, doi: 10.1109/ULTSYM.2019.8925905.

[6] Li, M. H., Chen, C. Y., Lu, R., Yang, Y., Wu, T., & Gong, S. (2019). Temperature Stability Analysis of Thin-Film Lithium Niobate SH0 Plate Wave Resonators. Journal of Microelectromechanical Systems, 28(5). https://doi.org/10.1109/JMEMS.2019.2934126

[7] Gong, S., Lu, R., Yang Y., Gao, L., Hassanen A. E. (2021). Microwave Acoustic Devices: Recent Advances and Outlook. IEEE Journal of Microwaves. https:// 10.1109/JMW.2021.3064825.